Testing Gravitational Memory Generation with Compact Binary Mergers

Huan Yang and Denis Martynov

Phys. Rev. Lett. **121**, 071102 — Published 17 August 2018

DOI: 10.1103/PhysRevLett.121.071102

Testing gravitational memory generation with compact binary mergers

Huan Yang[1,2] and Denis Martynov[3,4]

[1]*Perimeter Institute for Theoretical Physics, Waterloo, ON N2L2Y5, Canada*
[2]*University of Guelph, Guelph, ON N2L3G1, Canada*
[3]*LIGO, Massachusetts Institute of Technology, Cambridge, MA 02139, USA*
[4]*School of Physics and Astronomy and Institute of Gravitational Wave Astronomy, University of Birmingham, Edgbaston, Birmingham B15 2TT, United Kingdom*

Gravitational memory is an important prediction of General Relativity, which is intimately related to asymptotic symmetries at null infinity and the so-called soft graviton theorem. For a given transient astronomical event, the angular distribution of energy and angular momentum fluxes uniquely determine the displacement and spin memory effect in the sky. We investigate the possibility of using the binary black hole merger events detected by Advanced LIGO/Virgo to test the relation between the source's energy emission and the gravitational memory measured on earth, as predicted by General Relativity. We find that while it is difficult for Advanced LIGO/Virgo, one-year detection of a third-generation detector network will easily rule out the hypothesis assuming isotropic memory distribution. In addition, we construct a phenomenological model for memory waveforms of binary neutron star mergers, and use it to address the detectability of memory from these events in the third-generation detector era. We find that measuring gravitational memory from neutron star mergers is a possible way to distinguish between different neutron star equation of state.

Introduction. With the recent detection of a binary neutron star (BNS) merger using both gravitational wave (GW) and electromagnetic telescopes [1–3], we are quickly entering the era of multi-messenger astronomy with GWs. Future GW observations will provide unprecedented opportunies to uncover physical information of those most compact, exotic objects (such as black holes and neutron stars) in our universe. Moreover, future detections will open an independent window to study cosmology [4, 5], and will be used to test various predictions of General Relativity [6–8], such as the gravitational memory effect [9–12].

Gravitational memory is an observable phenomenon of the spacetime. Conceptually, it can be classified into ordinary memory, which is due to the change of quadrupole moment for slowly-moving sources, and null memory [50] that comes from null fields propagating to null infinity [13, 14]. Similarly the analog of gravitational memory has also been found in Maxwell theory [15]. The GW memory has a direct relationship with soft-graviton charges at null infinity [16] (also see developments in Maxwell theory [17, 18]), which have quantum gravity partners. These partners may play a key role in solving the Black Hole Information Paradox [19, 20]. The memory effect is probably one of the few macroscopic, astrophysical observables that could be traced back to a quantum gravity origin (another example is "echoes from black hole horizon" [21]). Studying such classical observables is interesting because observational signatures of quantum gravity are normally expected at Planck scale.

The detectability of the displacement memory effect using ground, spaced-based detectors and pulsar-timing arrays has been discussed extensively in the literature [22–29]. In addition, understanding and verifying the relations between memory effects and associated energy/angular momentum emissions from the source is equally important, as these relations display striking similarities to Weinberg's soft-graviton theorem [30]. They have been written in various forms in different context. In this work we adopt the form suitable to describe the null displacement memory generated by GW energy flux [22]:

$$h_{jk}^{\rm TT(mem)}(T_d) = \frac{4}{d}\int_{-\infty}^{T_d} dt' \left[\int \frac{dE^{\rm GW}}{dt' d\Omega'} \frac{n'_j n'_k}{1-\mathbf{n}'\cdot\mathbf{N}} d\Omega'\right]^{\rm TT}, \tag{1}$$

where T_d is the time of detection, $h_{jk}^{\rm TT(mem)}$ is the memory part of the metric in transverse-traceless gauge, $\frac{dE^{\rm GW}}{dt' d\Omega'}$ is the GW energy flux, $\mathbf{n}'$ is its unit radial vector and $\mathbf{N}$ is the unit vector connecting the source and the observer (with distance d).

We propose to use binary black hole (BBH) merger events to test the validity of Eq. (1). For any single event, a network of detectors is able to approximately determine its sky location and the intrinsic source parameters such as black hole masses, spins, and the orbital inclination by applying parameter estimation algorithms. The displacement memory effect, being much weaker than the oscillatory part of the GW signal, can also be extracted using the matched-filter method. By computing the GW energy with source parameters within the range determined by parameter estimation, we can obtain the value of the right-hand side of Eq. (1) and compare it with the measured displacement memory. Multiple events are need to accumulate statistical significance for such a test [31, 32].

As an astrophysical application for gravitational memory, we also examine the memory generated by BNS mergers with a simple, semi-analytical memory waveform

model. This memory waveform has a part that is sensitive to the star's equation of state (EOS) and post-merger GW emissions. Therefore we are able to study the possibility of using memory detection to distinguish different NS EOS in the era of third-generation detectors.

Memory distribution. For BBH mergers at cosmological distances, the memory contribution can be well approximated by [25, 33] [51] [52]:

$$h_+^{(\rm mem)} = \frac{\eta M_z}{384\pi d}\sin^2\iota(17+\cos^2\iota)h^{\rm mem}(T_d)\,, \quad (2)$$

where $M = m_1 + m_2$ is the total mass of the binary, z is the redshift, $M_z = M(1+z)$ is the redshifted total mass, $\eta = m_1 m_2/M^2$ is the symmetric mass ratio, ι is the inclination angle of the orbit. The posterior distribution of these source parameters can be reconstructed by performing Markov-Chain Monte-Carlo parameter estimation for each event. $h^{\rm mem}$ can be well modelled by the minimal-waveform model discussed in [25]. The angular dependence shown in Eq. (2) encodes critical information about the memory generation described by Eq. (1). It is maximized for edge-on binaries, which is different from the dominant oscillatory signals with $h_+ \propto (1+\cos^2\iota)$, $h_\times \propto \cos\iota$ dependence. In this work, we test the consistency of Eq. (2) with future GW detections as a way to test the memory generation formula Eq. (1). In particular, we test the ι-angle dependence [53] by formulating this problem in a Bayesian model selection framework.

Model test. We consider two hypotheses, with $\mathcal{H}_1$ resembling Eq. (2) and $\mathcal{H}_2$ describing an isotropic memory distribution in the source frame:

$$\begin{aligned}\mathcal{H}_1 &: h_+^{(\rm mem)} = \frac{\eta M_z}{384\pi d}\sin^2\iota(17+\cos^2\iota)h^{\rm mem}(T_d) \equiv h_{m1}\,,\\ \mathcal{H}_2 &: h_+^{(\rm mem)} = \frac{\eta M_z}{96\pi d}\sqrt{\frac{3086}{315}}h^{\rm mem}(T_d) \equiv h_{m2}\,, \end{aligned} \quad (3)$$

where the numerical coefficient of $h_+^{(\rm mem)}$ in $\mathcal{H}_2$ is chosen such that the (source) sky-averaged SNR^2 (signal-to-noise ratio) is the same for these two hypotheses. For each detected BBH merger event, the source parameters are described by

$$\theta^a = (\ln\mathcal{M}_z, \ln\eta, \chi_A, t_c, \phi_c, \ln d, \alpha, \delta, \psi, \iota)\,, \quad (4)$$

where $\mathcal{M}_z \equiv M_z\eta^{3/5}$ is the redshifted chirp mass, $\chi \equiv (m_1\chi_1 + m_2\chi_2)/M$ is the effective spin parameter [34] with χ_A representing the dimensionless spin of the Ath body, t_c and ϕ_c are the coalescence time and phase, α, δ and ψ are the right ascension, declination and polarization angle in the Earth fixed frame. Given a data stream y, to perform the hypothesis test, we evaluate the Bayes factor

$$\mathcal{B}_{12} = \frac{P(y|\mathcal{H}_1)}{P(y|\mathcal{H}_2)}\,. \quad (5)$$

In addition, the evidence $P(y|\mathcal{H}_i)$ is

$$P(y|\mathcal{H}_i) = \int d\theta^a P(\theta^a|\mathcal{H}_i)P(y|\theta^a\mathcal{H}_i)\,, \quad (6)$$

where the prior $P(\theta^a|\mathcal{H}_i)$ is the prior distribution of θ^a which is set to be flat, and the likelihood function is given by

$$\begin{aligned}\log P(y|\theta^a\mathcal{H}_i) &\propto -2\int df \frac{|y-h_{\rm IMR}-h_{mi}|^2}{S_n(f)}\\ &\equiv -\frac{||y-h_{\rm IMR}-h_{mi}||^2}{2}\,, \end{aligned} \quad (7)$$

with $h_{\rm IMR}$ the inspiral-merger-ringdown waveform and S_n the single-side detector noise spectrum. Both $h_{\rm IMR}$ and h_{mi} (cf. Eq. (3)) are functions of $\{\theta^a\}$. According to the derivation in the Supplementary Material, after performing the integration in Eq. (6), the log of this Bayes factor can be approximated by

$$\begin{aligned}\log\mathcal{B}_{12} \approx &-\frac{1}{2}||y-h_{\rm IMR}(\hat\theta)-\epsilon h_{m1}(\hat\theta)||^2\\ &+\frac{1}{2}||y-h_{\rm IMR}(\hat\theta)-\epsilon h_{m2}(\hat\theta)||^2\,. \end{aligned} \quad (8)$$

Here $\{\hat\theta^a\}$ are the Maximum Likelihood Estimators for $\{\theta^a\}$ using the IMR waveform template (PhenomB [34] is adopted in this work). Similar to [31, 32, 35], we denote the distribution of $\log\mathcal{B}_{12}$ in Eq. (8) as *foreground* or *background* distributions, assuming hypothesis 1 or 2 is true respectively. Given a detected event, these *foreground* and *background* distributions can be used to obtain the detection efficiency $P_{\rm d}$ and the false alarm rate $P_{\rm f}$ [31, 32, 35]. Given an underlying set of source parameters $\theta_0 = \{\theta_0^a\}$, the false alarm rate can be obtained if the detection efficiency is known. In this work we follow the convention in [36] and choose $P_{\rm d} = 50\%$.

For multiple events with data stream $\{y^{(i)}\}$, the combined Bayes factor is

$$\mathcal{B}_{12} = \prod_i \frac{P(y^{(i)}|\mathcal{H}_1)}{P(y^{(i)}|\mathcal{H}_2)}\,, \quad (9)$$

and the above discussion generalizes trivially because these events are independent. It turns out that, if we define $\mathrm{SNR}_{\rm eff}^{50\%}$ such that

$$P_{\rm f}^{50\%} = \frac{1}{\sqrt{2\pi}}\int_{\mathrm{SNR}_{\rm eff}^{50\%}}^{\infty} e^{-x^2/2}\,dx\,, \quad (10)$$

this effective SNR is given by

$$\mathrm{SNR}_{\rm eff}^{50\%} = \frac{\sum_i ||h_{m2}^{(i)}(\theta_0) - h_{m1}^{(i)}(\theta_0)||_i^2}{\sigma}\,, \quad (11)$$

with

$$\begin{aligned}\sigma^2 &= \sum_i \left\{||h_{m2}^{(i)}(\theta_0) - h_{m1}^{(i)}(\theta_0)||_i^2 + A_a^{(i)}(\Gamma_{ab}^{(i)})^{-1}A_b^{(i)}\right\}\,,\\ \Gamma_{ab}^{(i)} &= \langle\partial_{\theta^a}h_{\rm IMR}^{(i)}|\partial_{\theta^b}h_{\rm IMR}^{(i)}\rangle_i\,,\\ A_a^{(i)} &= \langle\partial_{\theta^a}h_{m1}^{(i)}|h_{m1}^{(i)}(\theta_0) - h_{m2}^{(i)}(\theta_0)\rangle_i\,, \end{aligned} \quad (12)$$

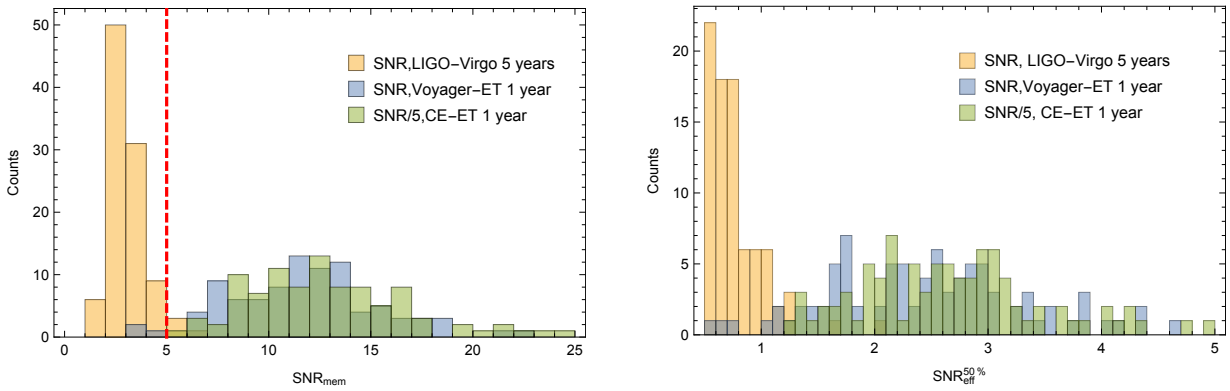

FIG. 1: Left panel: The distribution of the combined SNR of the gravitational memory for all events with expected memory SNR greater than 0.1, following a five-year observation period with a network of GW detectors containing Advanced LIGO (Livingston and Hanford) and Advanced Virgo at design sensitivities. As a comparison, we also plot the combined SNRs for the same set of events assuming third-generation detectors with a one-year observation period. The red dashed line highlights one commonly used detection threshold. Right panel: The inferred $\mathrm{SNR}_{\mathrm{eff}}^{50\%}$ for distinguishing the two hypotheses in Eq. (3) for the same set of detectors and with the same period of observation.

and the inner product is defined as

$$\langle\psi|\chi\rangle_i \equiv 2\int df \frac{\psi(f)\chi^*(f)+h.c.}{S_{n_i}(f)}\,. \tag{13}$$

The source parameter uncertainties enter into this hypothesis test result through the $A\Gamma^{-1}A$-type terms in Eq. 12. Because of the simplified treatment adopted in this analysis to save computational costs for simulated data, they are obtained essentially by the Fisher-Information method (Γ is the Fisher-Information matrix). In principle, the whole procedure can also be performed using Markov-Chain Monte-Carlo method, where the posterior probability distribution of each parameter can be more accurately computed.

Monte-Carlo source sampling. In order to investigate the distinguishability between different hypotheses within a given observation period, we randomly sample merging BBHs using a uniform merger rate in comoving volume $55\mathrm{Gpc}^{-3}\mathrm{yr}^{-1}$ [37]. The primary mass m_1 of the binary is sampled assuming a probability distribution $p(m_1)\propto m_1^{-2.35}$, where the secondary mass is uniformly sampled between $5M_\odot$ and m_1. We also require that an upper total mass cut-off $M<80M_\odot$ [38]. The effective spin χ_A is sampled evenly within $|\chi_i|<1$. The right ascension, declination, and inclination angles are randomly sampled assuming uniform distribution on the Earth's and source's sky. We perform 100 Monte-Carlo realizations, with each realization containing all BNS mergers within $z<0.5$ range (further binary merger events are too faint for memory detections) for one or five years.

The results of the Monte-Carlo (MC) simulation are shown in Fig. 1. We assume a detector network with Advanced LIGO (both Livingston and Hanford sites) and Advanced Virgo, with all detectors reaching design sensitivity. After five-year observation time, we collect all events with expected memory SNR above 0.1 for each MC realization, and compute the corresponding $\mathrm{SNR}_{\mathrm{eff}}^{50\%}$ as defined in Eq. (3). With a five-year observation, the median of this astrophysical distribution locates at $\sim 0.65\sigma$ level, which is insufficient to claim a detection. Therefore under the current best estimate of merger rate and with the assumed binary BH mass distribution, during the operation period of Advanced LIGO-Virgo, it is unlikely to distinguish the (source) sky distribution of the memory term as depicted by Eq. (1), (2) and an isotropic memory distribution. In comparison, we apply the Voyager (or Cosmic Explorer, CE) sensitivity to both LIGO detectors, and the Einstein Telescope (ET) sensitivity to the Virgo detector, and plot the corresponding SNR in Fig. 1. This shows that these 3rd-generation detector networks are fully capable of distinguishing these hypotheses. Our hypothesis test framework can also be applied to test against other memory distributions as well, by replacing the second line of Eq. (3) by the target hypothesis.

We also include the distribution of the combined SNR: $\mathrm{SNR}_{\mathrm{mem}}=\sqrt{\sum_i(\mathrm{SNR}_{\mathrm{mem}}^{(i)})^2}$ [54]. This can be achieved by stacking the memory terms from different events coherently, as explained in [23]. Its magnitude roughly reflects the strength of the combined memory signal over noise. Fig. 1 shows that $\mathrm{SNR}_{\mathrm{mem}}\sim 3$ may be achieved after five-year observation time. Similar SNR has been claimed in [23] with ~ 35 GW150914-like events and randomized sky locations, assuming single-detector sensitivity of Advanced LIGO.

Recovering the angular dependence. With a set of detections, it is also instructive to reconstruct the posterior angular dependence of memory, which can be compared with its theoretical prediction. Without loss of

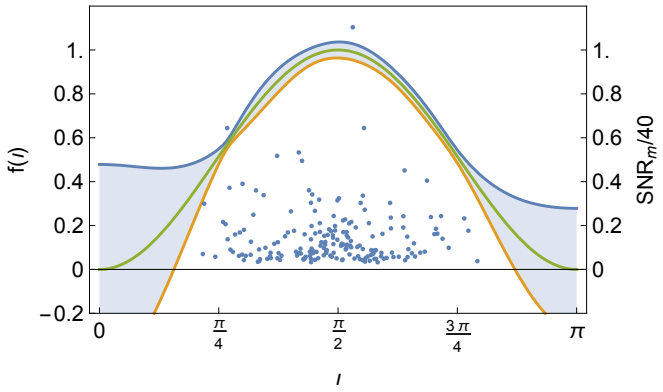

FIG. 2: The 1σ uncertainty (bound by the blue and yellow line) of angular dependence $f(\iota)$ reconstructed from a set of simulated events, as indicated by the shaded region. The green line presents the underlying angular distribution in Eq. (2). The SNR and ι of simulated events are presented by the dots in the plot.

generality, we parametrize the memory waveform as

$$h_+^{(\rm mem)} = \frac{17\eta M_z}{384\pi d} h^{\rm mem}(T_d) f(\{a_n, b_n\}, \iota)\,,$$
$$f(\{a_n, b_n\}, \iota) = \sum_{n=0}^{N} (a_n \sin n\iota + b_n \cos n\iota)\,, \qquad (14)$$

where N is the truncation wave number and $h^{\rm mem}(T_d)$ is a normalized Post-Newtonian waveform in the early inspiral stage. Given a set of observed events y_j, one can obtain the posterior distribution of a_i, b_i using Bayes Theorem ($a_0 = 0$):

$$P(\{a_i, b_i\}|\{y_j\}) = \frac{P(\{y_j\}|\{a_i, b_i\}) P(\{a_i, b_i\})}{P(\{y_j\})}\,, \qquad (15)$$

where the detailed expression for the likelihood function $P(\{y_j\}|\{a_i, b_i\})$ is explained in the Supplementary Material. In Fig. 2, we simulate observed events (with $\rm SNR_m \geq 1$) for a one-year period assuming CE-ET sensitivity. For simplicity, we assume that the memory distribution respects parity symmetry, such that all the a_i's are zero. The cutoff N is set to be 4. Based on the posterior distribution of the angular distribution parameter b_i, we compute the reconstructed uncertainty of f_ι at 1σ level, as depicted by the shaded area in Fig. 2.

Binary neutron stars. In addition to BBHs, merging BNSs also generate gravitational memory. However, given that NS masses are smaller than the typical BH masses in binaries and that the merger frequency is outside of the most sensitive band of current detectors, directly detecting the gravitational memory from BNS mergers is difficult for second-generation detectors.

Since the BNS waveform (especially the post-merger part) depends sensitively on the EOS, it is natural to expect that the detection of memory can be used to distinguish between various EOS. To achieve this goal, we have formulated a *minimal-waveform* model for BNS mergers similar to the construction for BBHs (see Supplementary Material). This model employs the fitting formula for post-merger waveforms developed in [39] to compute $dE^{\rm GW}/dt$ (c.f. Eq. (1)) in the post-merger stage, and a leading-PN description for the energy flux in the inspiral stage. For illustration purpose, we also consider four sample EOS studied in [39]: GNH3, H4, ALF2 and Sly. Assuming a $1.325M_\odot + 1.325M_\odot$ BNS system at distance 50Mpc away from Earth and following the maximally emitting direction, the SNRs for detecting these memory waveforms with Advanced LIGO are all around 0.1, which are insufficient to study the EOS of NSs. On the other hand, if we assume Cosmic Explorer (CE) sensitivity, the corresponding SNRs will be 10.1, 9.6, 8.9, and 10.4 respectively.

For third-generation GW detectors such as CE, the inspiral waveform of BNS can be used to determine source parameters (such as ι) to very high accuracies. For a $1.325M_\odot + 1.325M_\odot$ BNS system at distance 50Mpc [55], Fisher analysis suggests that the measurement uncertainty of ι is of order 10^{-2}. An accurate determination of source parameters breaks the degeneracy of amplitude between different BNS memory waveforms. We shall compute

$$\rm SNR_{\Delta ab} = \sqrt{4\int_0^\infty df\, \frac{|\tilde{h}^{\rm mem}_{\rm MWM,a} - \tilde{h}^{\rm mem}_{\rm MWM,b}|^2}{S_{\rm n,CE}}}\,, \qquad (16)$$

as a measure for distinguishability between arbitrary EOS a and b.

Following [40], if $\rm SNR_\Delta \leq 1$, we consider the two waveforms indistinguishable. The values listed in Table I indicate that measuring gravitational memory is a possible way to extract information about NS EOS. One unique advantage of this approach is that it is insensitive to the phases of post-merger modes, as the beating terms between modes generally contribute kHz modulation of $dE^{\rm GW}/dt$ or $h^{\rm mem}$, which is outside the most sensitive band of third-generation detectors [56]. Such mode phases still contain much more significant theoretical uncertainties than the mode frequencies in current numerical simulations.

Memory for ejecta. The electromagnetic observation of GW170817 provides strong evidence for the existence of multi-component ejecta [41, 42], which could originate

TABLE I: $\rm SNR_\Delta$ for various EOS.

EOS	GNH3	H4	ALF2	Sly
GNH3	0	1.3	5.2	3.8
H4		0	3.9	2.7
ALF2			0	2.3

from collisions of stars, wind from post-collapse disk [43], etc. Because of the transient nature, the GWs generated by ejecta(s) are likely non-oscillatory, and mainly composed of ordinary gravitational memory [44]:

$$h_{jk}^{\rm TT(mem)} = \Delta \sum_{A=1}^{N} \frac{4M_A}{d\sqrt{1-v_A^2}} \left[\frac{v_A^j v_A^k}{1-\mathbf{v_A}\cdot\mathbf{N}}\right]^{\rm TT} . \quad (17)$$

We shall phenomenologically write the ejecta waveform as $h_+ = h_0(1+e^{-t/\tau})^{-1}$, with the frequency domain waveform being $i\pi\tau/\sinh(2\pi^2 f\tau)$. Here τ characterizes the duration of the ejection process, and h_0 is the asymptotic magnitude of the memory. Depending on the angular distribution of ejecta materials, h_0 along the maximally emitting direction can be estimated as $h_0 \sim \Delta M v^2/d$, where ΔM is the ejecta mass and v is the characteristic speed. Assuming CE sensitivity, the SNR of such ejecta waveforms is a plateau for $\tau \leq 1$ms, and drops quickly for larger τ. The plateau value roughly scales as [57]

$$\mathrm{SNR}_{\rm ej} \sim 1.2 \left(\frac{\Delta M}{0.03 M_\odot}\right)\left(\frac{v}{0.3c}\right)^2 \left(\frac{d}{50\mathrm{Mpc}}\right)^{-1} . \quad (18)$$

In this case, a detection of the ejecta waveform is only plausible with information stacked from multiple events, and/or using detectors that achieve better low frequency sensitivity [45].

One can apply a similar analysis to the jet of a short gamma-ray burst [46]. The SNR roughly scales as $\sim 0.25(\Delta E_{\rm jet}/10^{51}\mathrm{erg})(50\mathrm{Mpc}/d)$, which is likely smaller. The neutrino radiation, as discussed in [47], can carry energy up to $\sim 10^{53}$erg, which could contribute significantly to the memory if the radiation is sufficiently anisotropic.

Conclusion. We have discussed two aspects of measuring gravitational memory in merging compact binary systems. BBHs are ideal to test the memory-generation mechanism, as a way to connect soft-graviton theorem and symmetry charges of the spacetime to astrophysical observables. BNSs can be used to distinguish between different NS EOS, as a complementary way to tidal Love number measurements in the inspiral waveform and (possibly) spectroscopy measurements of the post-merger signal. We have shown that both tasks may be achieved with the third-generation ground-based detectors.

Because of the $1/f$-type scaling of memory waveforms, improving the low-frequency sensitivity of detectors is crucial for achieving better memory SNR. This will be particularly useful for gravitationally probing the ejecta(s) produced in BNS mergers. Another interesting direction is to further explore the detectability and application of memory in space-based missions, such as LISA or DECIGO.

Acknowledgments. We would like to thank Haixing Miao and Lydia Bieri for fruitful discussions. We thank Beatrice Bonga and Yuri Levin for reading over the manuscript and making many useful comments. H.Y. is supported by NSERC and in part by Perimeter Institute for Theoretical Physics. Research at Perimeter Institute is supported by the Government of Canada through Industry Canada and by the Province of Ontario through the Ministry of Research and Innovation. D.M. acknowledges the support of the NSF and the Kavli Foundation.

[1] B. P. Abbott, R. Abbott, T. D. Abbott, F. Acernese, K. Ackley, C. Adams, T. Adams, P. Addesso, R. X. Adhikari, V. B. Adya, et al. (LIGO Scientific Collaboration and Virgo Collaboration), Phys. Rev. Lett. **119**, 161101 (2017), URL https://link.aps.org/doi/10.1103/PhysRevLett.119.161101.

[2] B. P. Abbott, R. Abbott, T. D. Abbott, F. Acernese, K. Ackley, C. Adams, T. Adams, P. Addesso, R. X. Adhikari, V. B. Adya, et al., The Astrophysical Journal Letters **848**, L12 (2017), URL http://stacks.iop.org/2041-8205/848/i=2/a=L12.

[3] B. P. Abbott, R. Abbott, T. D. Abbott, F. Acernese, K. Ackley, C. Adams, T. Adams, P. Addesso, R. X. Adhikari, V. B. Adya, et al., The Astrophysical Journal Letters **848**, L13 (2017), URL http://stacks.iop.org/2041-8205/848/i=2/a=L13.

[4] B. F. Schutz, Nature **323**, 310 (1986).

[5] L. S. Collaboration, V. Collaboration, M. Collaboration, D. E. C. G.-E. Collaboration, D. Collaboration, D. Collaboration, L. C. O. Collaboration, V. Collaboration, M. Collaboration, et al., Nature **551**, 85 (2017).

[6] N. Yunes, K. Yagi, and F. Pretorius, Physical review D **94**, 084002 (2016).

[7] E. Berti, K. Yagi, H. Yang, and N. Yunes, arXiv preprint arXiv:1801.03587 (2018).

[8] E. Berti, K. Yagi, and N. Yunes, arXiv preprint arXiv:1801.03208 (2018).

[9] Y. B. Zel'Dovich and A. Polnarev, Soviet Astronomy **18**, 17 (1974).

[10] L. Smarr, Physical Review D **15**, 2069 (1977).

[11] R. Bontz and R. Price, The Astrophysical Journal **228**, 560 (1979).

[12] D. Christodoulou, Physical review letters **67**, 1486 (1991).

[13] L. Bieri and D. Garfinkle, Physical Review D **89**, 084039 (2014).

[14] A. Tolish and R. M. Wald, Physical Review D **89**, 064008 (2014).

[15] L. Bieri and D. Garfinkle, Classical and Quantum Gravity **30**, 195009 (2013).

[16] T. He, V. Lysov, P. Mitra, and A. Strominger, Journal of High Energy Physics **2015**, 151 (2015).

[17] S. Pasterski, Journal of High Energy Physics **2017**, 154 (2017).

[18] P. Mao, H. Ouyang, J.-B. Wu, and X. Wu, Physical Review D **95**, 125011 (2017).

[19] S. W. Hawking, M. J. Perry, and A. Strominger, Physical review letters **116**, 231301 (2016).

[20] M. Mirbabayi and M. Porrati, Physical review letters **117**, 211301 (2016).

[21] V. Cardoso, S. Hopper, C. F. Macedo, C. Palenzuela, and

P. Pani, Physical Review D **94**, 084031 (2016).
[22] K. S. Thorne, Physical Review D **45**, 520 (1992).
[23] P. D. Lasky, E. Thrane, Y. Levin, J. Blackman, and Y. Chen, Physical review letters **117**, 061102 (2016).
[24] L. O. McNeill, E. Thrane, and P. D. Lasky, arXiv preprint arXiv:1702.01759 (2017).
[25] M. Favata, The Astrophysical Journal Letters **696**, L159 (2009).
[26] M. Favata, in *Journal of Physics: Conference Series* (IOP Publishing, 2009), vol. 154, p. 012043.
[27] M. Favata, Classical and Quantum Gravity **27**, 084036 (2010).
[28] R. Van Haasteren and Y. Levin, Monthly Notices of the Royal Astronomical Society **401**, 2372 (2010).
[29] D. Pollney and C. Reisswig, The Astrophysical Journal Letters **732**, L13 (2010).
[30] A. Strominger, arXiv preprint arXiv:1703.05448 (2017).
[31] H. Yang, K. Yagi, J. Blackman, L. Lehner, V. Paschalidis, F. Pretorius, and N. Yunes, Physical Review Letters **118**, 161101 (2017).
[32] H. Yang, V. Paschalidis, K. Yagi, L. Lehner, F. Pretorius, and N. Yunes, Physical Review D **97**, 024049 (2018).
[33] L. Bieri, D. Garfinkle, and N. Yunes, arXiv preprint arXiv:1706.02009 (2017).
[34] P. Ajith et al., Phys. Rev. Lett. **106**, 241101 (2011), 0909.2867.
[35] J. Meidam, M. Agathos, C. Van Den Broeck, J. Veitch, and B. S. Sathyaprakash, Phys. Rev. **D90**, 064009 (2014), 1406.3201.
[36] B. Abbott, R. Abbott, T. Abbott, F. Acernese, K. Ackley, C. Adams, T. Adams, P. Addesso, R. Adhikari, V. Adya, et al., arXiv preprint arXiv:1710.09320 (2017).
[37] B. Abbott, R. Abbott, T. Abbott, M. Abernathy, F. Acernese, K. Ackley, C. Adams, T. Adams, P. Addesso, R. Adhikari, et al., Physical Review X **6**, 041015 (2016).
[38] S. E. Woosley and A. Heger, in *Very Massive Stars in the Local Universe* (Springer, 2015), pp. 199–225.
[39] S. Bose, K. Chakravarti, L. Rezzolla, B. Sathyaprakash, and K. Takami, arXiv preprint arXiv:1705.10850 (2017).
[40] L. Lindblom, B. J. Owen, and D. A. Brown, Physical Review D **78**, 124020 (2008).
[41] G. Hallinan, A. Corsi, K. Mooley, K. Hotokezaka, E. Nakar, M. Kasliwal, D. Kaplan, D. Frail, S. Myers, T. Murphy, et al., Science p. eaap9855 (2017).
[42] S. Smartt, T.-W. Chen, A. Jerkstrand, M. Coughlin, E. Kankare, S. Sim, M. Fraser, C. Inserra, K. Maguire, K. Chambers, et al., Nature **551**, 75 (2017).
[43] D. M. Siegel and B. D. Metzger, Physical review letters **119**, 231102 (2017).
[44] V. B. Braginsky and K. S. Thorne, Nature **327**, 123 (1987).
[45] H. Yu, D. Martynov, S. Vitale, M. Evans, B. Barr, L. Carbone, K. L. Dooley, A. Freise, P. Fulda, H. Grote, et al., arXiv preprint arXiv:1712.05417 (2017).
[46] L. Bieri, P. Chen, and S.-T. Yau, Classical and Quantum Gravity **29**, 215003 (2012).
[47] L. Bieri and D. Garfinkle, in *Annales Henri Poincaré* (Springer, 2015), vol. 16, pp. 801–839.
[48] C. Talbot, E. Thrane, P. D. Lasky, and F. Lin, arXiv preprint arXiv:1807.00990 (2018).
[49] H. Miao, H. Yang, and D. Martynov, arXiv preprint arXiv:1712.07345 (2017).
[50] This includes the Christodoulou memory for GWs.
[51] This angular dependence assumes dominant (2,2) mode emission of GWs. The contribution from higher order modes is discussed in [48].
[52] $h_{\times}^{\rm mem}$ is zero for circular orbit and standard choice of polarization basis.
[53] In principle we could also test the dependence of memory amplitude versus other source parameters, such the factor before $\sin^2\iota$ in Eq. (2). In the Bayesian model selection framework, such dependence can be compared to a null hypothesis, where the amplitude is zero, in which case it becomes a memory detection problem. We refer interested readers to [23] for related discussions.
[54] In order to coherently stack different data sets to boost the SNR of the stacked memory term, one needs to measure the high-order modes of the inspiral waveform to determine the signs of the memory terms in advance [23]. For hypothesis tests discussed in this work, such measurement is not required.
[55] Here we assume CE sensitivity for Handford, Livingston and Virgo detectors.
[56] Unless it is a high-frequency detector targeting kHz band, such as the one discussed in [49].
[57] We assume that the lower cut-off frequency for computing SNR is 5Hz.